Turkish J. Eng. Env. Sci.
33 (2009) , 159 – 166.

doi:10.3906/muh-0904-11

An energy absorption comparison of square, circular, and elliptic steel and aluminum tubes under impact loading

Javad MARZBANRAD[1], Mehdi MEHDIKHANLO[2] , Ashkan SAEEDI POUR[2]
School of Automotive Engineering, Iran University of Science and Technology, Tehran-IRAN
e-mail: marzban@iust.ac.ir, mehdikhanlo@auto.iust.ac.ir, ashkan_357@yahoo.com

Received 24.04.2009

Abstract

By carrying out finite element simulation, energy absorption values of thin-walled tubes with different geometric dimensions were investigated. Square, circular, and elliptic tubes of steel and aluminum were used to compare energy absorption. The experimental results of load-displacement used for verification in the square steel tubes showed good agreement. Three-dimensional simulation was accomplished with a finite element method while the impactor collided with one side of tube and the other side was kept rigid. Square tubes for 2 specified widths with 2 different thicknesses were also compared. In addition, 2 other cross sections including circle and ellipse with the same area were studied for comparison in a load-displacement curve. The results show that the ellipse cross section had more energy absorption than the 2 others. Moreover, the amount of energy absorption will be greater with increasing thickness for smaller section tubes.

Key Words: Impact, Energy absorption, Finite element method, Axial crushing.

Introduction

The axial folding of metal tubes has been known for several decades as an excellent energy absorbing mechanism. Today, components based upon this principle are utilized in high-volume industrial products such as cars, trains, and other sectors where energy, during a crush situation, needs to be absorbed in a controlled way (Hanssen et al., 2001). Investigation of crushing energy absorption is very important and is expected from the point of safety design of passenger vehicle (Yamazaki and Han, 1998). Shell structures are used in many engineering applications due to their efficient load carrying capability relative to material volume (Reid et al., 1984;; Reid et al., 1989; Reid, 1993; Marzbanrad et al., 2006). Since thin-walled sections are one of the most efficient energy absorbing components of an automobile, axial crushing of thin-walled tubes has long been the subject of extensive research (Abramowicz and Jones, 1984; Peixinho et al., 2003; Schneider and Jones, 2004; ;arzbanrad et al., 2009a; Marzbanrad et al., 2009b). To absorb the impact energy effectively, a material is required to exhibit an extended stress plateau. Thus, enhancement of the absorbed energy can be achieved by increasing the plateau strain (Miyoshi et al., 1999). The predominant domain of applications of collapsible energy absorbers is that of crush protection. Axi-symmetric and circular shapes provide perhaps the widest range of all choices for use as absorbing elements because of their favorable plastic behavior under axial forces, as well as their common occurrence as structural elements. However, less attention has been given to the study of square tubes to be used as energy absorbers. The quasi-static axial crush response of a thin-wall, stainless steel box component has been extensively studied to isolate the effect of alloy composition and microstructure on the axial crush configuration response (DiPaolo et al., 2004) and the axial crush configuration response of thin-wall, steel box components has been studied for the specific axial crush configuration response of steel, square box components under quasi-static testing conditions (;ohnson and Reid, 1978; Reid and Reddy, 1986; Babbage and Mallick, 2004; DiPaolo and Tom, 2006). The results of the present study are compared with the available experimental results (Aljawi et al., 2004). Typical corresponding load-displacement curves are presented. Good agreement was achieved between the experimental and finite element studies.

Formulation

There are 2 main types of impact: elastic and plastic. The impacting phenomenon between the impactor and the part that is a tube in this study could be complicated since transient and nonlinear analyses are involved. These tubes could be used in automotives as bumper stays for absorption of energy. Absorption of energy for these parts has a vital role during a vehicle crash to enhance passenger's safety. A plastic impact involves a significant amount of energy dissipated in the collision. An impact between 2 vehicles or between 1 vehicle and a rigid body, where the vehicles crumple on impact, is an example of an elasto-plastic impact. A principle of energy conservation in the elastic impact is governed; the kinetic energy before impact is conserved and converted to elastic energy and the kinetic energy of the impactor and the automobile at its maximum deflection, i.e.

$$\frac{1}{2}M_A V_A^2 = \frac{1}{2}M_A V_0^2 + \frac{1}{2}M_B V_0^2 \tag{1}$$

where M_A is mass, of impactor, M_B is the mass of vehicle, V_A is the velocity of the impactor before impact, and V_0 is the final velocity of the impactor and vehicle in maximum deflection point. An important consideration of momentum is that it can be neither created nor destroyed. Thus the momentum before an impact is equal to the momentum after the impact. At the moment of its maximum deflection, a principle of momentum conservation before and after impact can be expressed as follows:

$$M_A V_A = (M_A + M_B)\, V_0. \tag{2}$$

After the separation point, energy and momentum conservation equations can be expressed as follows:

$$\frac{1}{2}M_A V_A^2 = \frac{1}{2}M_A V_{A2}^2 + \frac{1}{2}M_B V_{B2}^2 \tag{3}$$

$$M_A V_A = (M_A V_{A2} + M_B V_{B2}) \tag{4}$$

where V_{A2} and V_{B2} are the final velocities of the impactor and vehicle, respectively, at the separation point. In the elastic-plastic impact, the principle of linear momentum conservation is satisfied, since impact forces are equal and opposite as shown in Eq. (5).

$$M_A V_A + M_B V_B = (M_A V_{A2} + M_B V_{B2}) \tag{5}$$

In this case, the velocities after impact may be determined with the coefficient of restitution (e). The coefficient of restitution (COR) is the ratio of speed of separation to speed of approach in a collision as Eq. (6).

$$e = \frac{V_{B2} - V_{A2}}{V_A - V_B} \tag{6}$$

An object with a COR equals to 1 collides elastically, while an object with a COR of 0 will collide inelastically, effectively sticking to the object it collides with, not bouncing at all. The coefficient of restitution is a number that indicates how much kinetic energy (energy of motion) remains after a collision of 2 objects. If the coefficient is high (very close to 1), it means that very little kinetic energy was lost during the collision. If the coefficient is low (close to zero), it suggests that a large fraction of the kinetic energy was converted into heat or was otherwise absorbed through deformation. Equation (7) can be used to find the energy dissipated, ED, during an impact. This is found by subtracting the kinetic energy of the 2 masses after impact, and the kinetic energy of the impactor before impact.

$$E_{\text{Plastic}} = \frac{1}{2}M_A V_A + \frac{1}{2}M_B V_B = \frac{1}{2}\left(M_{A2}V_{A2} - M_{B2}V_{B2}\right) \tag{7}$$

Modeling

In this study, LS-DYNA is employed to investigate the deformation of tubes under dynamic loading conditions. Some various choices of impact elements can be considered like implicit and explicit models. Here, nonlinear explicit impact modeling elements are used for analysis.

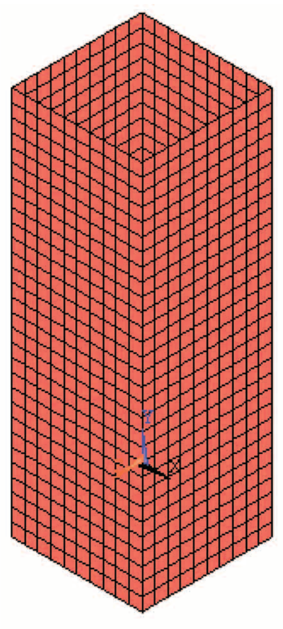

Figure 1. Three-dimensional model.

The tubes used in this study are of different widths and thicknesses but fixed lengths with a 3-dimensional model as shown in Figure 1. ANSYS software with an element type of "thin shell element" is used for modeling and LS-DYNA software for analysis. Constraints are imposed on reference nodes located at the tip of the upper and lower rigid surfaces.

Numerical parameters

Steel extruded square tubes studied in this research were of 2 different sizes. The mean widths of these 2 square tubes were 30 mm and 50 mm. Meanwhile, 2 wall thicknesses were considered here of 1.25 mm and 1.5 mm; while length was kept at 150 mm. Tables 1 and 2 show the tube dimensions and material properties of the metal used in this paper. Considering axial compression, the load-displacement curves for these tubes with different geometries (square, circle and ellipse) were obtained. This study was carried out with an impact mass of 100 kg and a maximum impact speed of 9.396 m/s. For the present simulation, a purely kinematic hardening model was fitted to the steel and aluminum extruded material with the mechanical properties presented in Table 2 and underwent reverse loading as isotropic plasticity with the standard Von-Mises yield criterion and an associated flow rule.

Table 1. Square tubes parameters.

thickness (mm)	length (mm)	width (mm)
1.25	150	30
1.5	150	30
1.25	150	50
1.5	150	50

Table 2. Mechanical properties.

	E (GPa)	Y (MPa)	ν	ρ(kg/m^3)
Steel	207	280	0.3	7830
Aluminum	70	20	0.33	2700

Results and Discussion

Figure 2 shows the load history for a square tube with a width of 30 mm. Figure 3 represents the load history for a square tube with a width of 50 mm. Good agreement and almost full conformance can be observed between the maximum force of experimental and the present study's results for both square tubes. In the experimental method (Ajawi et al., 2004), the impact load applied to the square tube and the load-displacement graph achieved are illustrated here for comparison. They were used for verification of the simulation to establish the reliability of further results with different cross sections.

It is observed from Figure 2 that the results of the present study are lower than the experimental results and the difference between them is about 17% at the peak of the diagram. However, in some parts of this diagram the difference is less than 17% or without considerable differences. Figure 2 reveals that the first experimental peak-load has a shift relative to the predicted values. This may be attributed to the initial post-buckling behavior of the tube, which occurs at large plastic strains. Figure 2 also shows that the 2 curves are somehow the same with little non-conformity in the range of 5-10 mm and 15-25 mm displacements. This may be related to the size of meshing or the type of used material.

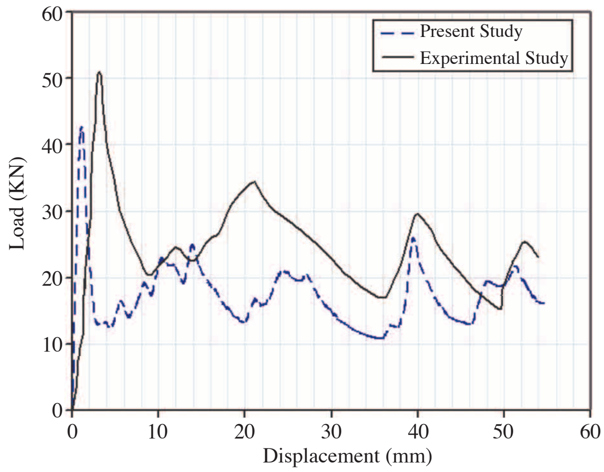

Figure 2. Load-displacement curves for a 30 × 30 mm square tube (1.25 mm thickness).

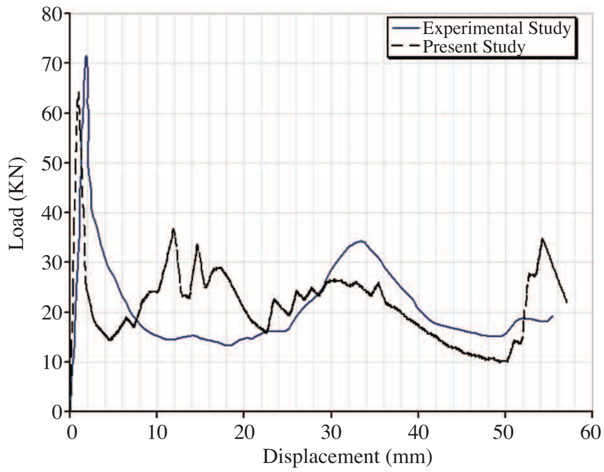

Figure 3. Load-displacement curves for a 50 × 50 mm square tube (1.25 mm thickness).

The same results are observed from Figure 3 with non-conformity in the range of 8-20 mm displacements. In this figure, it can be observed that the experimental and simulated results have 10% differences, indicating that the simulated results could be approximated for tests in non-conservative cases. It may be also concluded from Figures 2 and 3 that the energy absorption may be increased about 22% with width enhancement of 66%, showing that the energy absorption would be one-third of the width increase. Energy absorption was calculated from the area of the curve beneath the load-displacement.

Moreover, the thickness was studied for a specified cross section. Figure 4 shows the load history for a square tube with a width of 30 mm and with 2 different thicknesses. From this figure, it is observed that an increase in thickness of about 20% caused a 50% increase in energy absorption.

Figure 5 also represents the load-displacement history for a 50 mm square tube with 2 different thicknesses, i.e. 1.25 mm and 1.5 mm. It shows that with an increase in thickness of 20% there will be an increase in energy absorption of about 25%. It is concluded from Figures 4 and 5 that the amount of energy absorption will be greater with increasing thickness for smaller section tubes.

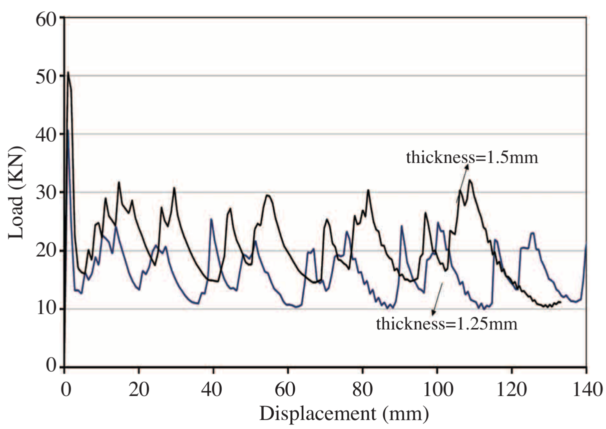

Figure 4. Load-displacement curve for a 30 × 30 mm square with 2 thicknesses.

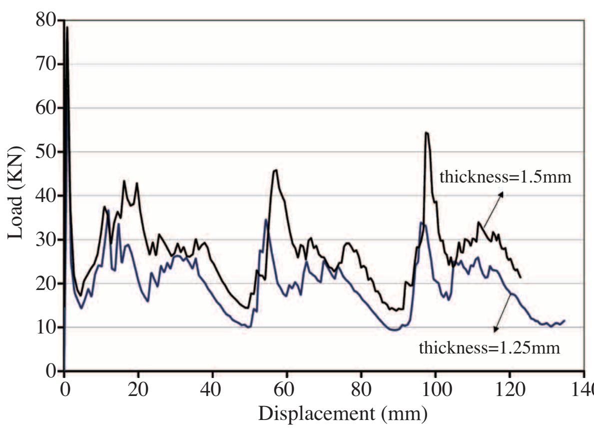

Figure 5. Load-displacement curves for a 50 × 50 mm square tube with 2 thicknesses.

In this research, difference between energy absorption of three different geometries has been also studied. Square, circle, and ellipse as shown in Figure 6 with the same area and thickness (1.5 mm) and the same height (150 mm) used here for comparison of load-displacement diagrams.

Figure 6. Square, circle, and ellipse tubes.

Figure 7 demonstrates the shapes predicted using finite element developed models. In this figure, the penetration time is 0.018 s for all 3 cases.

Figure 7. Simulation of shapes predicted.

As can be seen from Figure 7 a complete description of the collapse process is involved in several stages. That is, when compression started, the first fold usually tended to form outwards from the 2 opposite sides of the tube and inwards from the other 2. The folds started with a load peak rise rapidly higher than the other peaks, until the tube sides collapsed. The load then decreased rapidly to the first local minimum, in which the first outward and inward flattening folds were fully developed. That is, folding of the walls started in the vicinity of one end of the tube. The second increase in the load could be observed after the first folding of the walls ended, i.e. contact of the walls started, leading to formation of the second folding of the adjacent walls. Then the second drop of the load occurred again, indicating the second folding of the walls. Thus, the load dropped when new folding started, and rose when the walls came in contact. This process was repeated until the folding of the tube was completed showing the behavior of the crushed tube as a rigid body. In addition, the material of tubes was investigated in the impact loading. For this case, steel and aluminum were used for comparison in 3 sectional items. Figures 8 and 9 show the load-displacement of square, circular, and elliptic steel and aluminum tubes, respectively. These tubes have the same dimensions in area, thickness, and height.

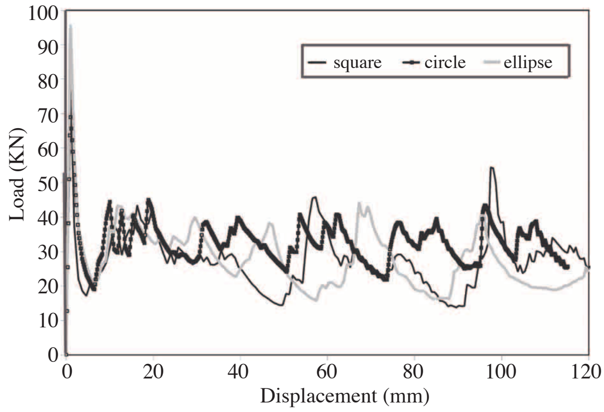

Figure 8. Load-displacement of square, circle and elliptic steel tubes.

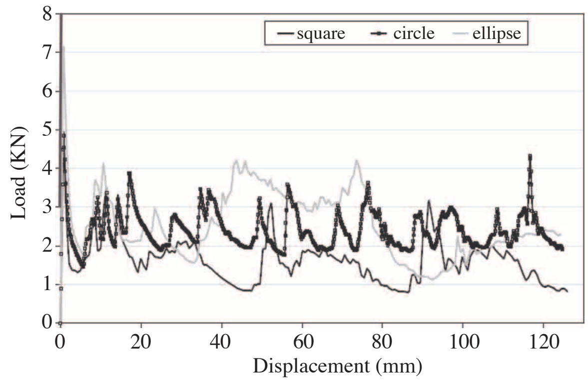

Figure 9. Load-displacement of square, circle, and elliptic aluminum tubes.

As is inferred from Figure 8, the energy absorption of the elliptic tube is 33% and of the circle tube is 17% more than that of the square tube.

The comparison of these aluminum tubes shows that the elliptic section is 50% and circular section is 33% greater than the square section tube in terms of energy absorption. Figures 8 and 9 show that the amount of energy absorption per weight of steel tube is 4.5 times greater than for the aluminum tube for all 3 sections. However, the square section and then the circular section of steel tube absorbed energy per weight more than the elliptic section of the aluminum tube, respectively.

Conclusion

In this paper, axial crushing of steel and aluminum tubes between 2 parallel plates subjected to impact dynamic axial loading was investigated. A nonlinear finite element model was developed and analyzed with LS-DYNA in this simulation. Verification was done through comparison with some experimental results in a steel square tube. Good agreement was observed between the FEM force histories with those obtained from experimental results. Typical deformation histories for 3 sectional types (square, circle, and ellipse) were studied and presented. It was concluded that the elliptic tubes absorb more energy during collisions. The effects of width and thickness were also investigated. It was concluded that the energy absorption may be increased about 22% with width enhancement of 66%, showing that the energy absorption would be one third of the width increase. Related to thickness, the amount of energy absorption will be more with increasing thickness for smaller section tubes. Energy per weight absorption during the collision of 2 metals (steel and aluminum) was also calculated and compared. The results showed that the amount of energy absorption per weight of steel tube was about 4.5 times greater than the aluminum tube for all 3 sections, square, circle and ellipse. However, the square section and then the circular section of the steel tube absorbed energy per weight more than the elliptic section of the aluminum tube, respectively.

Nomenclature

A	area of the tubes,	P	density
E	modulus of elasticity	M_A	mass of the impactor,
Y	yield stress	M_B	e mass of vehicle
V	velocity impactor	V_A	velocity of the impactor before impact

V_0	the final velocity of the impactor	V_{B2}	final velocities of the vehicle
Keq	the equivalent impact stiffness of a bumper	E	coefficient of restitution (COR)
V_{A2}	final velocities of the impactor		

References

Abramowicz, W. and Jones, N., "Dynamic Axial Crushing of Square Tubes", Int. J. Impact Eng., 2, 179-208, 1984.

Aljawi, A.A.N., Abd-Rabou, M. and Asiri, S., "Finite Element and Experimental Analysis of Square Tubes under Dynamic Axial Crushing", European Congress on Computational Methods in Applied Sciences and Engineering, 2004.

Babbage, J.M. and Mallick, P.K., "Static Axial Crush Performance of Unfilled and Foam-Filled Aluminum–Composite Hybrid Tubes ", Composite Structures 70, 177-184, 2005.

DiPaolo, B.P., Monteiro, P.J.M. and Gronsky, R., "Quasi-Static Axial Crush Response of a Thin-Wall, Stainless Steel Box Component" International Journal of Solids and Structures 41, 3707-3733, 2004.

DiPaolo, B.P. and Tom, J.G., "Study on an Axial Crush Configuration Response of Thin-Wall, Steel Box Components: The Quasi-Static Experiments", US Army Engineer Research and Development Center, Vicksburg, MS 39180, 2006.

Hanssen, A.G., Langseth, M. and Hopperstad, O.S., "Optimum Design for Energy Absorption of Square Aluminum Columns with Aluminum Foam Filler Structural Impact", International Journal of Mechanical Sciences, 43153-176, 2001.

Johnson, W. and Reid, S.R., "Metallic Energy Dissipating Systems", Applied Mechanics Reviews 31, 277-288, 1978.

Marzbanrad, J., Kamyab, A. and Mashadi, B., "Effect of Strain Rate, Module of Elasticity And Yield Point on Energy Absorption Behavior of Thin Cylindrical Shells", The 10^{th} World Automotive Congress, Fisita, Yokohama, Japan, F2006M208, p. 274, 2006.

Marzbanrad, J., Abdollahpour, A. and Mashadi, B., "Effects of Triggering of Circular Aluminum Tubes on Crashworthiness", International Journal of Crashworthiness, 14, 6, 591-599, 2009.

Marzbanrad, J., Alijanpour, M. and Kiasat, M.S., "Design and Analysis of an Automotive Bumper in Low-Speed Frontal Crashes", Journal of Thin-Walled Structure, 47, 902-911, 2009.

Miyoshi, T., Itoh, M., Mukai, T., Kanahashi, H., Kohzu, H., Tanabe, S. and Higashi, K., "Enhancement of Energy Absorption in a Closed Cell Aluminum by the Modification of Cellular Structures", Department of Metallurgy and Material Science, College of Engineering, Osaka Prefecture University, 1-1 Gakuen-cho, Sakai, Osaka, Japan. 599-8531, 1999.

Peixinho, N., Jones, N. and Pinho, A., "Experimental and Numerical Study in Axial Crushing of Thin Walled Sections Made of High-Strength Steels", Journal De Physique IV: JP, 110, 717-722, 2003.

Reid, S.R., "Plastic Deformation Mechanisms in Axially Compressed Metal Tubes Used as Impact Energy Absorbers", Int. J. Mech. Sci. 35: 1035-1052, 1993.

Reid, S.R., Reddy, T.Y. and Peng, C., "Dynamic Compression of Cellular Structures and Materials", In Structural Crashworthiness and Failure. Eds. N., Jones T., Wierzbicki. J. Wiley, New York, 1989.

Reid, S.R., Austin, C.D. and Smith, R., "Tabular Rings as Impact Energy Absorbers", Structural Impact and Crashworthiness, 2: 555-563, 1984.

Reid, S.R. and Reddy, T.Y., "Axially Loaded Metal Tubes as Impact Energy Absorbers", in: Inelastic Behavior of Plates and Shells – International Union of Theoretical and Applied Mechanics Symposium, Rio de Janeiro, Brazil. Springer-Verlag, Berlin, pp. 569-595, 1986.

Schneider, F. and Jones, N. "Impact of Thin-Walled High-Strength Steel Structural Sections", Proc. Intern. Mech. Engrs., Part D, J. Automobile Engineering, 218(2), pp. 131, 2004.

Yamazaki, K. and Han, J., "Maximization of the Crushing Energy Absorption of Tubes", Structural Optimization, 16, 37-46, 1998.